machines

MDPI

Article

Durability Comparison of SKD61 and FDAC Steel Mold Inserts in High-Pressure Die-Casting Process

Hai Nguyen Le Dang [1], Van-Thuc Nguyen [1], Van Huong Hoang [1], Xuan Tien Vo [1,*] and Van Thanh Tien Nguyen [2,*]

[1] Faculty of Mechanical Engineering, Ho Chi Minh City University of Technology and Education, Ho Chi Minh City 71307, Vietnam; hainld@hcmute.edu.vn (H.N.L.D.); nvthuc@hcmute.edu.vn (V.-T.N.); huonghv@hcmute.edu.vn (V.H.H.)

[2] Faculty of Mechanical Engineering, Industrial University of Ho Chi Minh City, Nguyen Van Bao Street, Ward 4, Go Vap District, Ho Chi Minh City 70000, Vietnam

* Correspondence: tienvx@hcmute.edu.vn (X.T.V.); nguyenvanthanhtien@iuh.edu.vn or thanhtienck@naver.com (V.T.T.N.)

Abstract: The high-pressure die-casting (HPDC) process involves injecting molten light metal into a steel mold under high pressure, resulting in parts with excellent surface quality and precise dimensions. However, this process subjects the mold to thermal fatigue and mechanical stress, which can lead to damage over time. This study investigated the wear characteristics of two types of inserts made from different steel materials, SKD61 steel and FDAC steel, under HPDC conditions. A thorough approach that combined computer simulations, experiments, and 3D scanning was employed to analyze wear patterns and dimensional changes after up to 300 casting cycles. The results indicate that the SKD61 steel outperformed the FDAC steel in terms of wear resistance and dimensional stability. The maximum deposition values of the SKD61 mold were only 0.009 mm, which was only 25% compared to the FDAC mold, indicating a significantly higher wear resistance. These findings are crucial for selecting and enhancing insert materials in HPDC, ultimately leading to higher-quality and more efficient casting.

Keywords: SKD61 steel; FDAC steel; mold durability; wear analysis

check for updates

Academic Editor: Kai Cheng

Received: 21 February 2025
Revised: 2 April 2025
Accepted: 14 April 2025
Published: 24 April 2025

Citation: Nguyen Le Dang, H.; Nguyen, V.-T.; Hoang, V.H.; Vo, X.T.; Nguyen, V.T.T. Durability Comparison of SKD61 and FDAC Steel Mold Inserts in High-Pressure Die-Casting Process. *Machines* **2025**, *13*, 352. https://doi.org/10.3390/machines13050352

Copyright: © 2025 by the authors. Licensee MDPI, Basel, Switzerland. This article is an open access article distributed under the terms and conditions of the Creative Commons Attribution (CC BY) license (https://creativecommons.org/licenses/by/4.0/).

1. Introduction

The high-pressure die-casting (HPDC) process involves injecting molten metals such as aluminum, brass, and magnesium or their alloys into a steel mold cavity under high pressure [1]. It is a popular manufacturing method for producing high-volume, high-precision, light-alloy components in the automotive, aerospace, and electronics sectors. This high pressure allows the metal to fill the mold cavity quickly, with flow velocities ranging from 3 m/s to 6 m/s, resulting in parts that boast excellent surface finishes and dimensional accuracy compared to other casting techniques [1,2]. However, the short cycle times expose the mold to significant thermal cycling and mechanical wear. The continuous heating and cooling of the mold, along with the abrasive characteristics of the high-pressure molten metal, contribute to the gradual deterioration of the mold material.

The lifespan of the steel mold and the inserts in the high-pressure die-casting (HPDC) process are essential factors in ensuring the casting components' shape, dimension quality, and durability. Guo et al. [2] studied metal–die interfacial heat-transfer coefficients in HPDC processes with the consideration of both the process parameters and casting thickness as well as alloys. The results also revealed that using ADC12 instead of AM50 allowed for closer contact between the casting and die, resulting in a higher interfacial heat-transfer

coefficient. Domkin et al. [3] focused on the direct modeling of high-temperature, diffusion-controlled die soldering in the aluminum high-pressure die-casting process. The simulation results showed that a higher strength and risk of soldering were projected to occur in "hot spot" sections of the die surface, consistent with observations in the literature. Queudeville et al. [4] discussed decision and design methodologies for the layout of modular dies in HPDC processes in another related study. A novel perspective on the value chain of HPDC dies was established. The layout of modular dies consists of an analysis of previously created die-cast molds.

The choice of materials and surface treatments plays a crucial role in determining the lifespan of these inserts. Research has thoroughly examined the performance of different tool steels used in high-pressure die-casting (HPDC) processes. For instance, SKD61 steel, a Japanese JIS grade known for its high hardness, excellent wear resistance, and thermal stability, shows remarkable resistance to thermal shock compared to FDAC or Ferrite-Austenite Dual-phase Cold-rolled steel. This characteristic is vital for preventing cracking during fast-paced production cycles, making SKD61 a preferred option for applications that demand precision and durability. Additionally, SKD61's performance can be further improved with PVD coatings, which help minimize reactivity with molten aluminum, thus prolonging tool life. On the other hand, FDAC steel is recognized for its excellent thermal conductivity and toughness, making it ideal for intricate die designs and high-volume production. Evaluating the performance of these steel inserts under high-pressure conditions offers valuable insights into their effectiveness for various applications within the die-casting industry. While FDAC steel is a more cost-effective choice with lower hardness, it is easier to machine and performs satisfactorily in specific applications.

The main wear mechanisms in HPDC are corrosion and thermal fatigue, and coatings such as chromium carbide have shown potential in reducing these issues [4–8]. Innovative methods for predicting fatigue life through thermal stress analysis have been developed, proving the reliability of SKD61 under different operational conditions [9]. Tsai et al. [10] applied the Taguchi method to enhance processing conditions for abrasive jet polishing of SKD61, which led to an improved surface finish and decreased wear. Similarly, Chen et al. [11] examined the tool wear characteristics of SKD61 during milling, confirming its strong resistance to thermal stress.

This research hypothesizes that the wear resistance of mold steels after many high-pressure die-casting cycles can be related to the surface hardness of the materials. Therefore, selecting suitable mold steels could improve the quality of the products. This study aims to address this gap by comprehensively comparing the two materials, FDAC and SKD61, under real-world HPDC conditions. It assesses the durability of mold cavities and cores made from these distinct materials by conducting a series of 300 die-casting cycles using the same casting parameters. The performance of the FDAC and SKD61 steels are evaluated in terms of wear resistance and dimensional stability. Furthermore, a simulation tool is employed to identify the optimal casting parameters and predict the wear patterns of the mold core and cavity throughout the casting process. The findings from this study will provide valuable insights for selecting suitable mold materials, ultimately enhancing production efficiency and reducing costs in HPDC processes.

2. Materials and Methodology

The research flowchart in Figure 1 outlines the research study steps. The details will be described later.

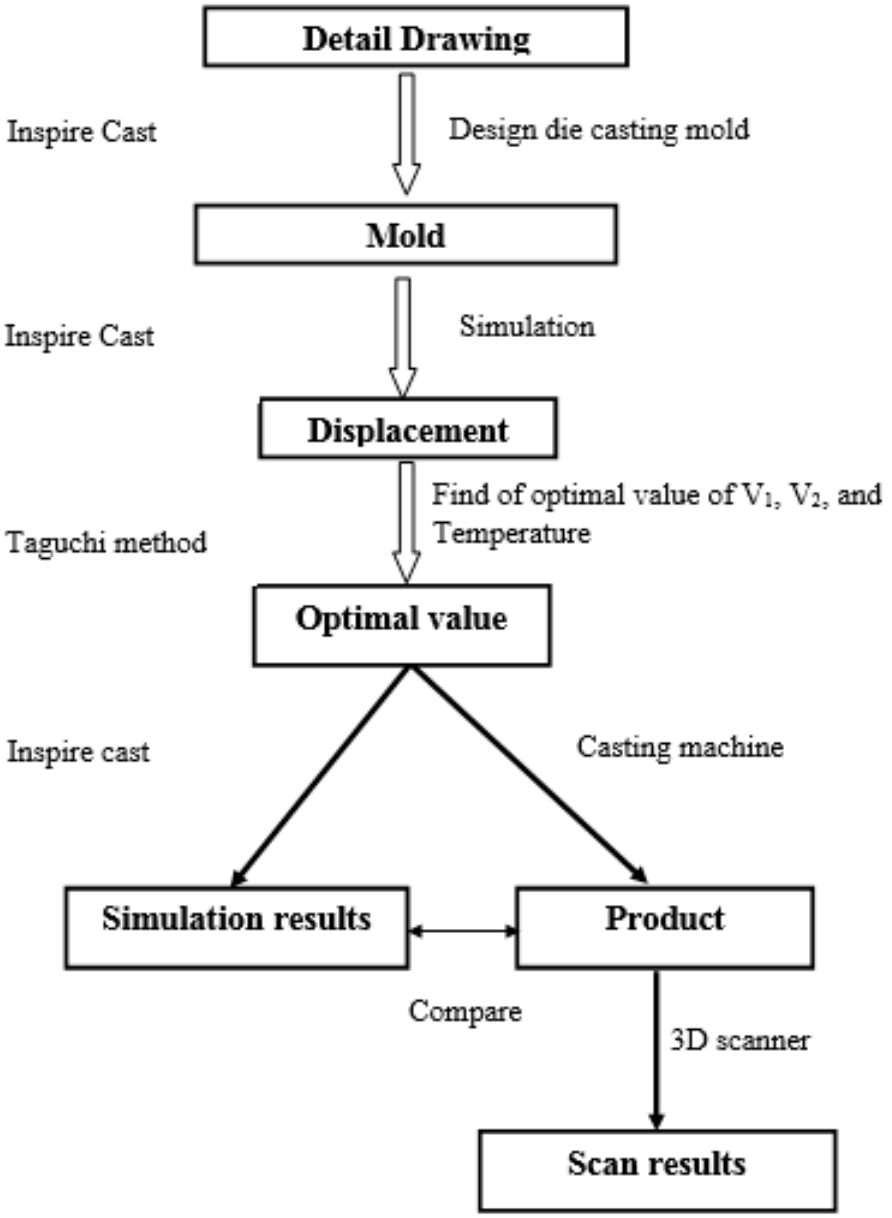
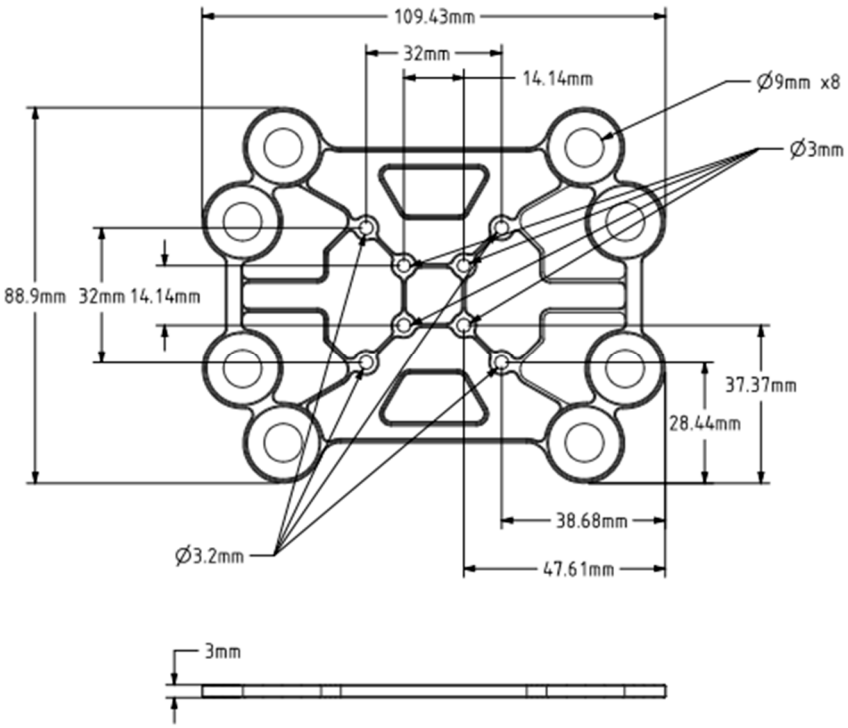


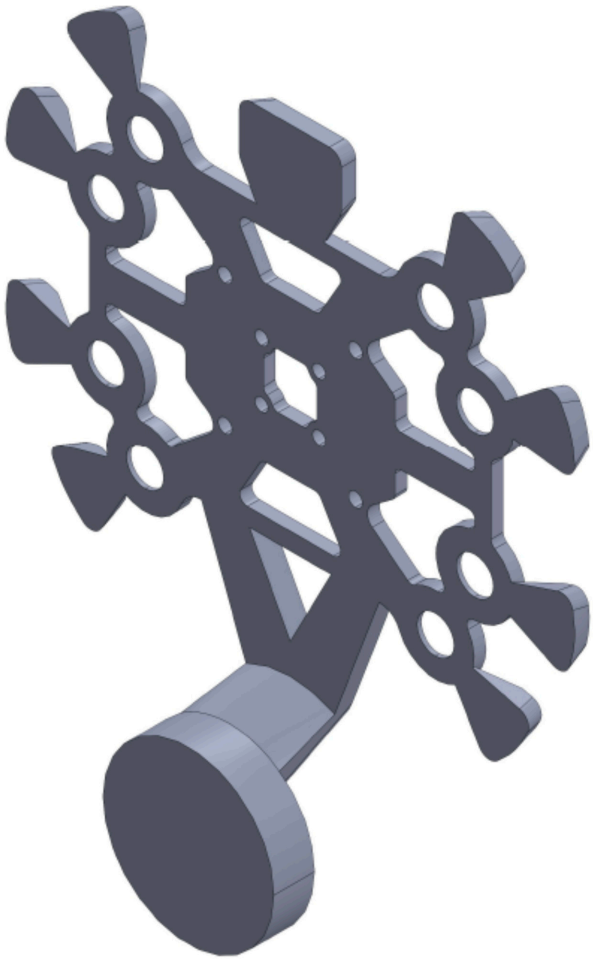
Figure 1. Research flowchart.

2.1. Mold Design and Material Choice

The drawing of a part shown in Figure 2a shows an item in an anti-vibration assembly for a camera drone. The part is thin, with an average thickness of 3 mm, has a thin rib along the boundary, has a symmetric shape, and is quite complex. All 3 mm holes were machined for installation with screws. The model's design, product material, and high-pressure die-casting process were fixed by an industrial partner, limiting our ability to modify it for easy casting. The solution for the limited budget was as follows: one shot produced one part. Camera drones require complex parts while maintaining a light weight, so ADC12 aluminum alloy was selected. The casting material used was ADC12 aluminum alloy, a widely used material in HPDC for its good mechanical properties and castability. In the first stage, the designed part was transferred into the casting model (Figure 2b), which had one leading runner, two branch runners, and two gates. Eight symmetric overflows and one overflow opposite the runner gate surrounded the part. Overflows were attached to ensure complete metal fill in the cavity and prevent porosity during die-casting.



(**a**)



(**b**)

Figure 2. Detailed drawing and casting: (**a**) detailed drawing; (**b**) casting.

This research required the use of two molds. A mold insert offers a cost-effective solution for reducing costs when producing a new mold. In addition to this, we cast the other parts with similar shapes and the total dimensions, so using an insert mold was the best solution. In this study, two types of steel, SKD61 and FDAC, were used to insert the mold into the molds, as shown in Figure 3. Both materials were chosen for their widespread use in HPDC mold manufacturing [6,12–15].

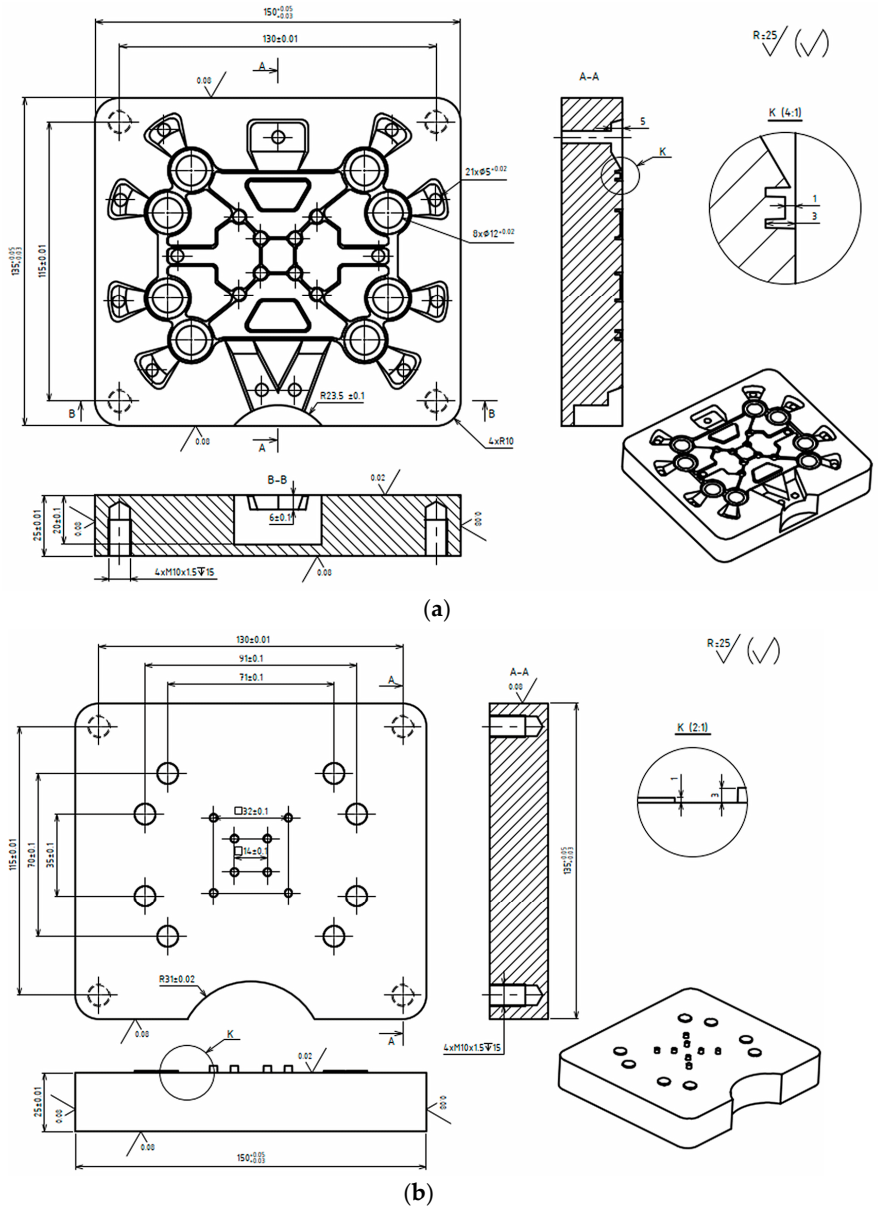


Figure 3. Core insert and cavity insert: (**a**) core insert; (**b**) cavity insert (unit: mm).

Table 1 shows the standard chemical composition ranges for SKD61 (JIS G4404) and FDAC (Phu Thinh Co., affiliated with Nippon Steel, Tokyo, Japan). The composition of SKD61 includes a high-alloy hot-work tool steel recognized for its exceptional resistance to wear, thermal fatigue, and deformation at elevated temperatures. This performance is attributed to its alloying elements, including carbon (C), chromium (Cr), molybdenum (Mo), and vanadium (V), which enhance its hardness and abrasion resistance. SKD61 steel has an initial hardness of around 48–52 HRC, which allows it to maintain its shape and resist deformation during casting operations. In addition, FDAC is a medium-grade tool steel that offers a lower hardness and is easier to machine and more cost-effective, making

it a practical choice for less-demanding applications. With a hardness range of 40–48 HRC, FDAC is pre-treated to enhance its load-bearing capacity and abrasion resistance. Its lower cost compared to SKD61 helps to reduce initial investments, making it suitable for production processes that do not require high temperature resistance while still delivering reliable performance. The differences in the chemical positions of the two steels lead to the differences in their mechanical properties. These characteristics are needed in molds. The mold inserts were installed into pressure-casting molds 300 times for test casting. The maximum number was limited to 300 due to budget constraints.

Table 1. The main chemical compositions of SKD61 steel and FDAC steel.

Element	C (%)	Cr (%)	Mo (%)	V (%)	Si (%)	Mn (%)	Fe (%)
SKD61	0.39	5.15	1.4	0.8	1.0	0.4	balance
FDAC	0.33–0.42	4.8–5.5	1.2–1.6	0.3–0.8	0.8–1.2	0.55–0.75	balance

2.2. Cold Chamber Casting Simulation

The independent parameters chosen as the input parameters have the most significant impact on the HPDC process. V1 is the first-phase velocity (slow-shot), i.e., the initial slow movement of the plunger used to push the molten metal past the pour hole and toward the gate. V2 is the second-phase velocity (fast-shot), i.e., the subsequent rapid acceleration of the plunger used to quickly fill the mold cavity. These are the critical parameters that influence the filling patterns, air entrapment, and pressure. The following parameters were chosen: the first-phase velocity (cap V sub 1), the second-phase velocity (cap V sub 2), and the temperature of the furnace. The first-phase velocity, typically ranging from 0.15 to 0.25 m/s, takes place in a fraction of a second and is essential for minimizing defects such as air entrapment and ensuring proper mold filling, and it thus significantly influences the quality of cast parts [15]. The second-phase velocity affects the interaction between the liquid metal and air during the mold-filling stage, thereby significantly impacting the final quality of cast components, and it can thus lead to defects such as gas porosity [16]. In the study by Advekar et al. [17], they used a pouring temperature that ranged from 660 °C–700 °C. These melting temperatures are higher than that of ADC12 aluminum (516 °C–582 °C), used for temperature compensation. The Taguchi method was used to optimize the casting parameters with three input parameters, each with three levels. Factor 1 was increased by 0.05 per step, factor 2 was increased by 0.5 per step, and factor 3 was increased by 50 per step. The factors and levels of the casting parameters are presented in Table 2. Some boundary conditions for the simulation process were constraints on the movement of the mold during casting, material flow limits at the gates, and heat transfer rates between the molten metal and mold material.

Table 2. Input parameters of this study.

	Parameter Value			
Parameters	**Parameter Level**			**Optimal Value**
V_1 (m/s)	0.15	0.2	0.25	0.25
V_2 (m/s)	1.5	2.0	2.5	1.5
T_{ADC12} (°C)	650	700	750	700

A lower signal-to-noise ratio (S/N) is better for minimizing the response [10]:

$$\frac{S}{N} = -10\log_{10}\left(\frac{1}{n}\sum_i^n y_i^2\right) \quad (1)$$

where y_i is the response value for the trial condition repeated n times. The S/N ratios were computed for nine trial conditions. S/N is the signal-to-noise ratio. The signal represents the desired outcome, such as minimal wear and consistent dimensional stability of the mold insert. Noise represents the variability caused by uncontrollable factors (e.g., inconsistencies in material flow and variations in the molten metal temperature).

As shown in Figure 4, the S/N ratio of factor 1 decreased from approximately 12 to about 11 at 0.25 as the level increased. The S/N ratio initially increased between 1.5 and 2.5. Factor 3 decreased and then increased. The optimal values are shown in the last column of Table 2. In this research, the signal-to-noise ratio was chosen according to the criterion of smaller being better in order to find the optimal value. This study chose the "smaller-is-better" criterion, which minimizes undesired results like wear, deformation, and defects, ensuring a longer lifespan and higher quality of the mold insert. According to the results shown in Table 2 and Figure 4, it was concluded that the first-phase velocity (V_1), second-phase velocity (V_2), and melting temperature T_{ADC12} (°C) values of 0.25 m/s, 1.5 m/s, and 700 °C, respectively, provided a suitable solution with the minimum simulation time.

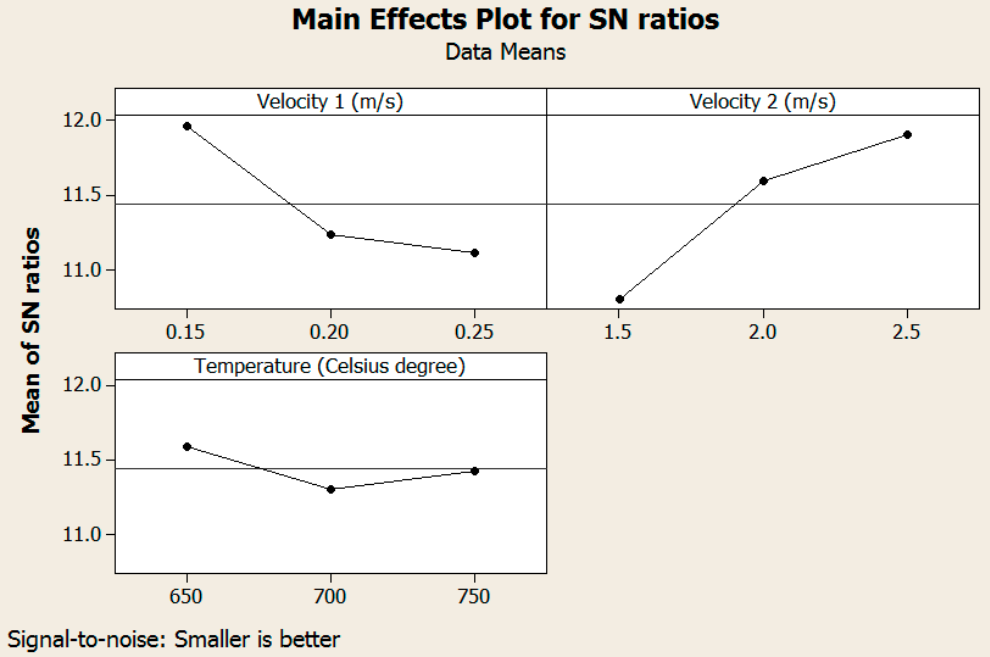


Figure 4. Optimal casting parameters.

2.3. Experimental Setup

Figure 5 shows the layout of the workshop floor, with the electric box on the right side, the induction furnace in the middle, the cooling tower (behind the furnace), and the horizontal-type YODA DC-100V5 (YOTA International Co., Ltd., Yongkang City, Tainan, Taiwan). The electric cabinet provided electricity both for the machine and the furnace. The furnace was positioned near the machine to reduce the distance travelled when pouring the metal. This cold chamber type required manual pouring. The machine had a piston with a diameter of 42 mm and a stroke length of 355 mm. During the experiment casting process, the first phase had a velocity of 0.15 m/s, the second phase had a velocity of 2.5 m/s, and the pouring temperature was 700 °C. Moreover, the experimental procedure is presented in Figure 1.



Figure 5. Horizontal-type casting machine with support facilities.

2.4. Measurement Method

In order to track the changes in the shape of the mold cavity and the mold insert, using a method that did not touch the surfaces was the best choice, mainly because of the mold's complex 3D design. Measurements were taken before any casting (as a baseline) and then again after every 100 casting cycles to see how the mold was wearing and changing in size.

A "GOM scan 1" 3D scanner from Carl Zeiss GOM Metrology GmbH company, Leipheim, Germany, was used, which employed structured light and followed the triangulation principle to capture images of the surfaces with a very high accuracy ($\pm$0.001 mm) without touching them. This scanner used the GOM software 2022 and Zeiss lenses. It had a laser that shone a line or pattern onto the measured surface. This laser light acted as a reference. The collected data were then used to create a 3D surface model, allowing for exact measurements of the wear and deformation. When the laser hit the surface, it returned to the scanner, where a sensor or camera picked up the reflected light. These scans showed the wear patterns and how much the surface had worn down. Both the mold core and cavity, made from SKD61 steel and FADC steel, were scanned 16 times in total. This helped in creating detailed 3D models of the objects, ensuring that their surfaces were not damaged. The results included parameters such as the height, surface comparison, flatness, and angles, though only a selection of these are presented in this article.

2.5. Simulation

The target parameters of these simulations were the filling time, die material temperature, material flow, material flow velocity, insert erosion, molding pressure, shrinkage, part displacement, and mold cavity temperature. At the same time, the simulation results also helped to point out defects in the mold cavity, such as air holes and weld lines.

3. Results and Discussion

3.1. Simulation Results

Figure 6 shows the molten fluid in blue vectors from the piston entering the biscuit, the leading runner, and two branch runners with laminar flow. However, the red vectors in the circle flow at the gate show the high velocity of melting fluid to fill the entire part. This caused severe wear at the gate and on the surface of the mold cavity insert. The location of the eight positioning pins on the cavity insert deformed over time, and the pin's tip was worn during the molding process. The surfaces of the inserts underwent corrosion throughout the casting process. The inserts tended to have a downward displacement, creating a large but shallow crater.

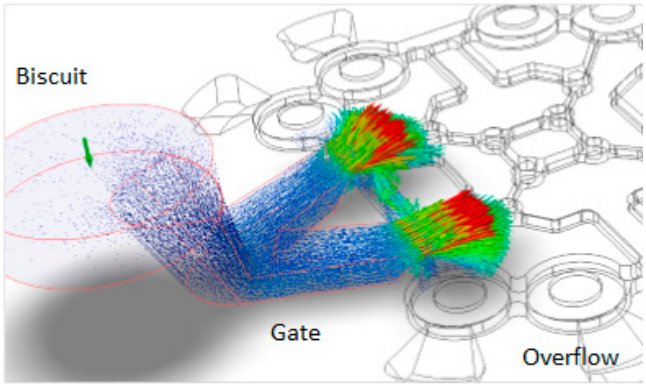


Figure 6. The flow pattern of the melted aluminum.

3.2. Three-Dimensional Scanning Results

One disadvantage of 3D scanning is that it is costly. However, its results can provide greater accuracy.

3.2.1. Surface Comparison of Core Insert

The observed fluctuations in the deposition/erosion values at the specific tracing point were due to the complex and competing wear mechanisms co-occurring in the HPDC process, such as thermal fatigue, erosion corrosion/soldering, and plastic deformation.

The scenario shown in Figures 7–10 highlights critical insights into the deformation and deposition characteristics of the core inserts after multiple shots. Deformation took place on all the surfaces of the insert. However, some locations eroded faster than others. Figure 7 points out some locations where substantial deformation of the insert material occurred, indicating the areas most susceptible to wear and stress. Figure 8 displays the core insert scan results of the two materials. The line graphs shown in Figures 9 and 10 present the point value measurements extracted from Figure 8. Figure 9 provides the measured variation in the deposition values on the FDAC core insert, offering a quantitative view of the material build-up across the surface. Figure 10 presents similar data for the SKD61 core insert, allowing for a comparative assessment of the deposition behavior between the different insert materials.

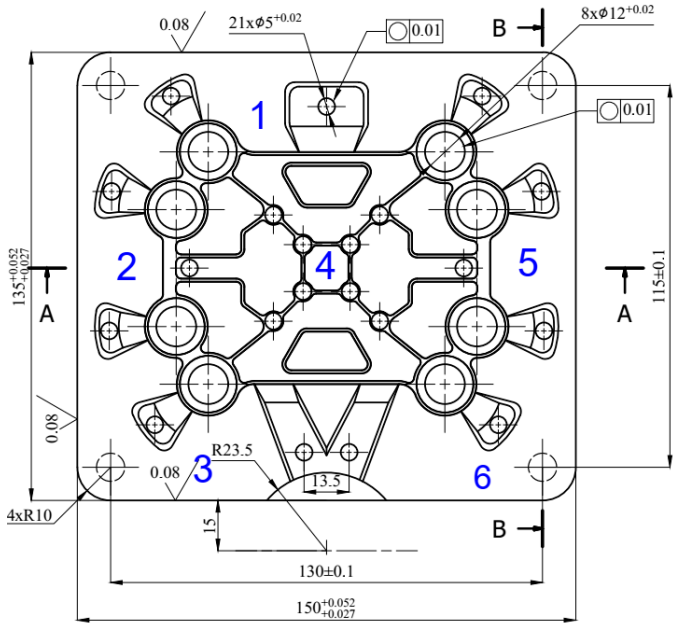


Figure 7. Six tracing points on the core insert (unit: mm).

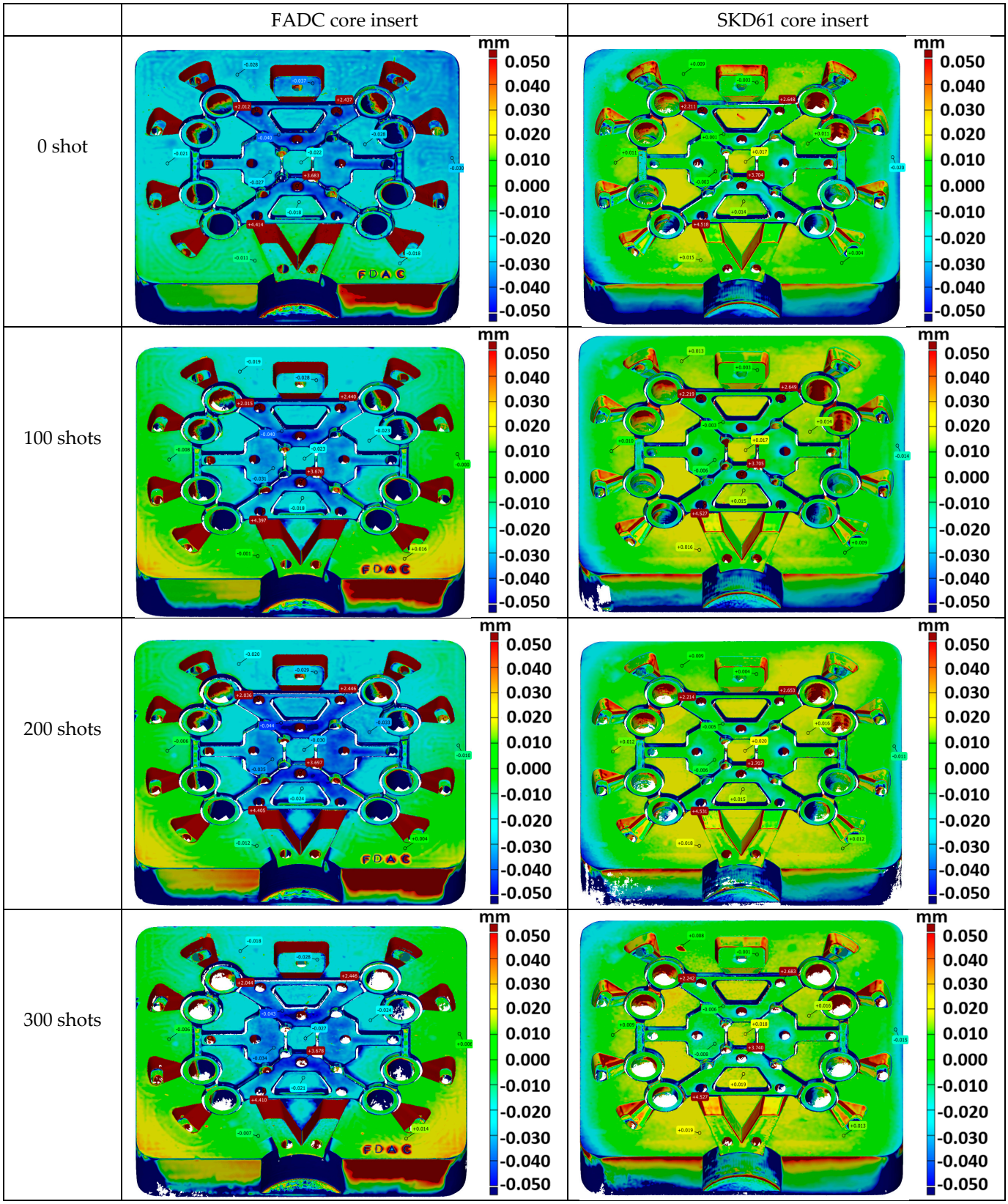


Figure 8. Three-dimensional scanning results of FADC core (**left**) and SKD61 core (**right**) insert every 100 shots.

Figure 9 shows the variation in the values of the depositions on the FDAC core inserts. As shown in Figure 7, the first, second, and third positions were located along the edges of the mold core and showed a displacement trend that generally moved upward, though

the variation remained minimal. At the fifth and sixth positions and at the edges of the core, the displacement trend was upward as well. Notably, the fifth position exhibited the highest deformation value in the cavity, which could be up to 0.036 mm. In contrast, the fourth position in the central area displayed a downward trend in displacement when compared to its original state.

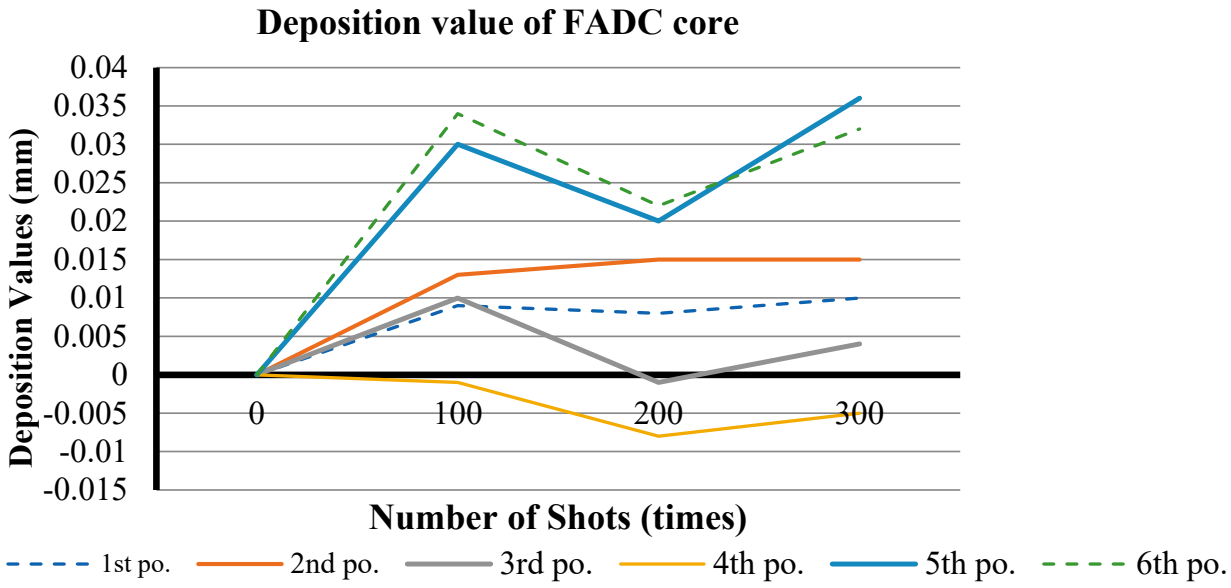


Figure 9. Variation in values of depositions on FDAC core insert.

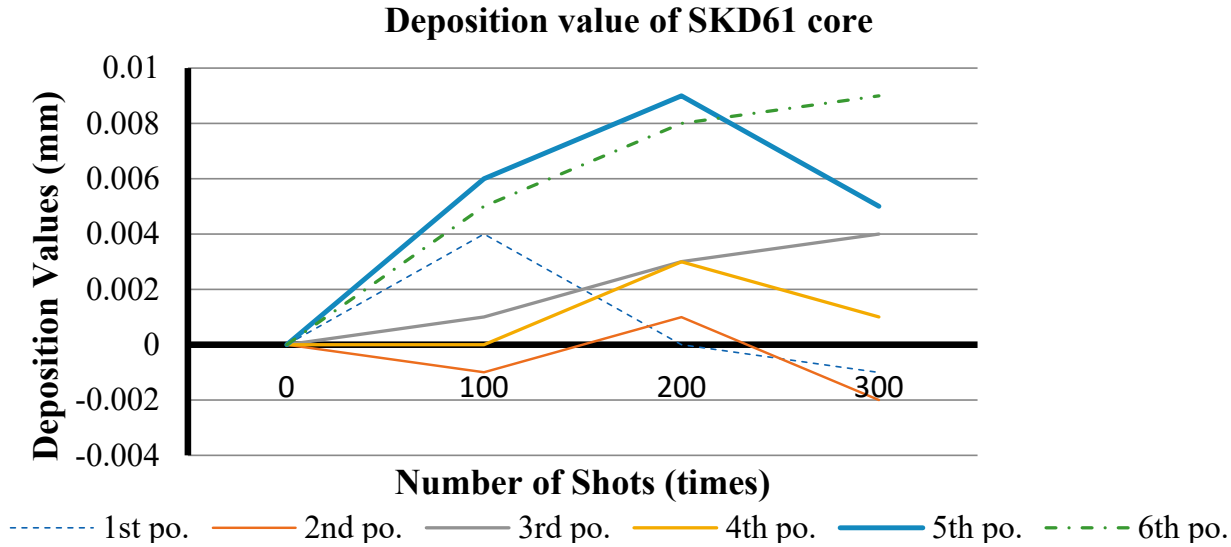


Figure 10. Variation in values of depositions on SKD61 core insert.

Figure 10 shows the variation in the values of the depositions on the SKD61 core inserts. The displacement values at the traced locations demonstrated unpredictable variations throughout the casting process. However, the variation values did not change significantly after 300 castings. The results show that the fourth position, which was at the center of the mold core, demonstrated no significant changes after 300 castings and that these tended to be convex. For the fifth and sixth positions, which were at the edge positions of the mold core, the line representing the displacement variation had a trend in the upward direction. At the sixth position, the core deformation value was the highest, which could be up to 0.009 mm.

Discussion 1:

After 300 castings, the SKD61 core insert was more stable than the FDAC mold insert. The maximum deposition values of the SKD61 mold were only 0.009 mm, which was only 25% compared to the FDAC mold, indicating a significantly higher wear resistance. The reason for this phenomenon could be the higher surface hardness of the SKD61 core insert. At the fifth and sixth positions, both mold cores had identical changes. The mold core tended to show changes in convex displacement values. At the fourth position in the core of the FDAC mold, there was a tendency for concave displacement to remain in the core of the mold; the displacement at the fourth position of the SKD61 mold remained unchanged after the casting process. The third position was near the runner. The FDAC mold core was more stable in this position than the SKD61 mold core.

3.2.2. Surface Comparison of Cavity Insert

Figure 11 displays six locations where significant deformation of the insert occurred after the shots. Figure 12 shows the variation values of the depositions on the FDAC cavity insert; Figure 13 shows the SKD61 cavity insert.

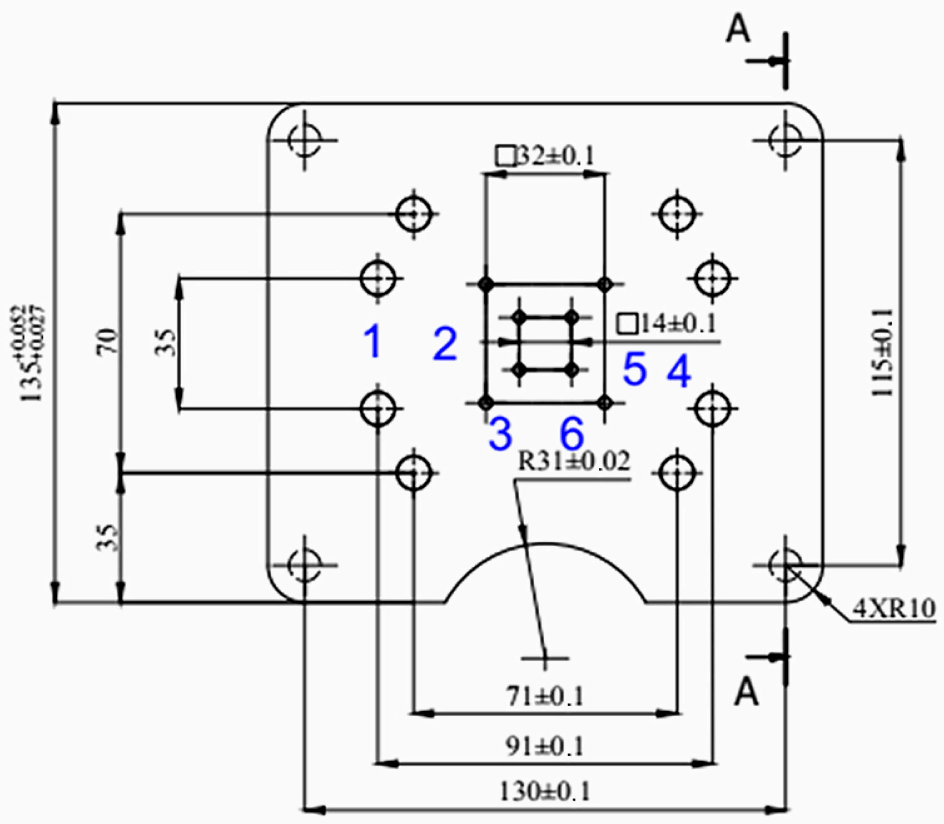


Figure 11. Six tracking points on the cavity insert (unit: mm). Positions 1, 2, 3, 4, 5, and 6 in Figure 11 indicate the measurement locations.

Figure 12 displays the scanning images of the two materials. The point value measurements are presented in Figures 13 and 14.

As shown in Figure 13, after 300 castings, the FDAC mold cavity was worn out. The third and sixth positions were the positions that suffered the most wear, which could reach −0.012 mm, followed by the second and fifth positions, which were also subject to abrasion and were significantly worn. The first and fourth positions were the least worn positions; no grinding occurred when they were worn out. The forming rods on the mold cavity were also significantly eroded.

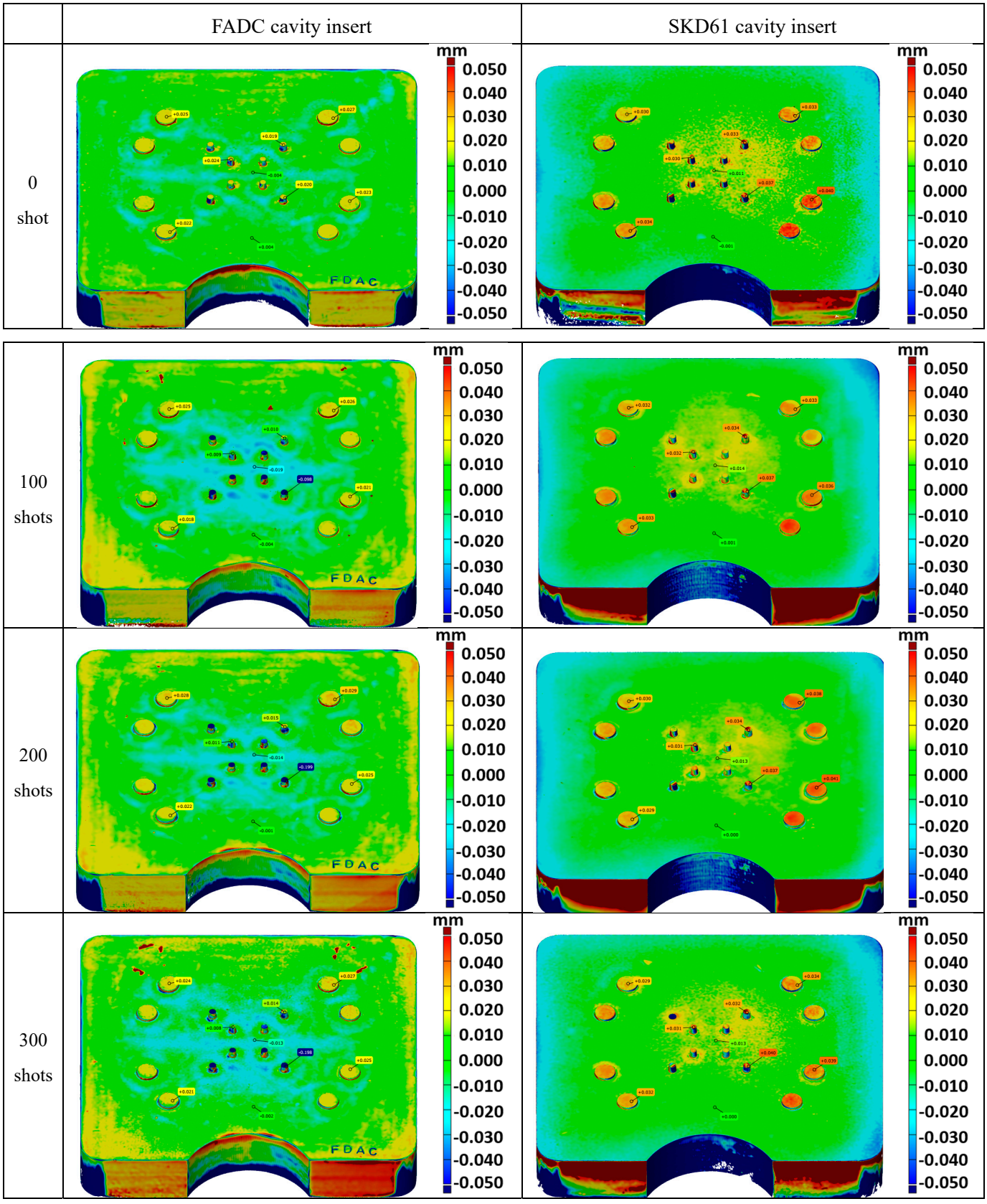


Figure 12. Three-dimensional scanning results of FDAC cavity (**left**) and SKD61 cavity (**right**) before casting and after each 100 shots.

As shown in Figure 14, after 300 castings, the SKD61 mold cavity was eroded, but the erosion value was not significant. The third and sixth positions were the most susceptible

to wear, but after 300 castings, erosion did not seem to occur. The fourth and fifth positions were the positions with the highest level of wear after 300 castings on the SKD61 mold cavity. The shaping rods on the mold cavity also did not have too much wear. The second position 2 had the most significant deposition value, which could reach −0.007 mm.

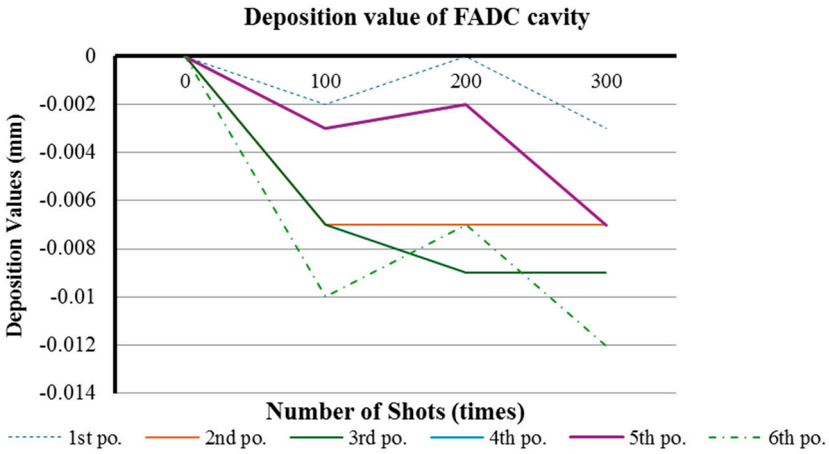


Figure 13. Variation in values of depositions on FDAC cavity insert.

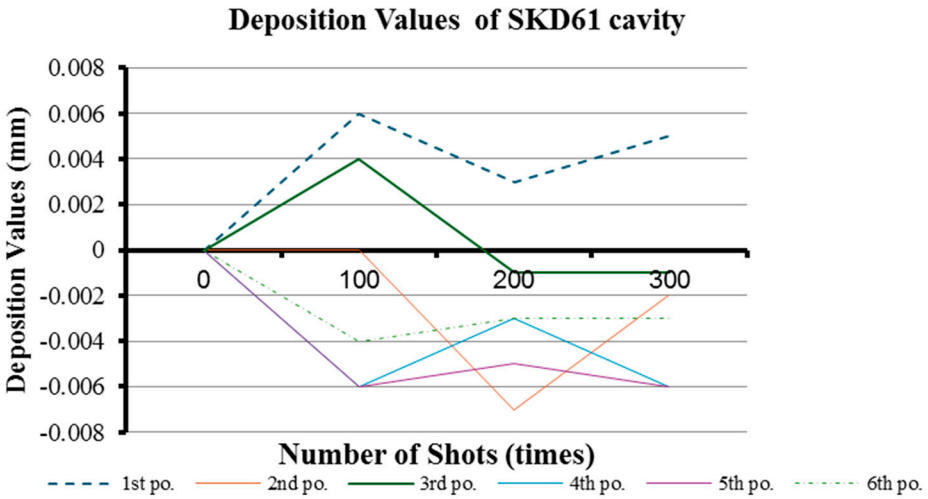


Figure 14. Variation in values of depositions on SKD61 cavity insert.

Discussion 2:

After 300 castings, the FDAC mold cavity exhibited greater wear than the SKD61 mold cavity. The third and sixth positions were the positions subject to the most significant wear. The forming rods on the FDAC mold cavity were eroded, while those on the SKD61 mold cavity were not.

3.3. Defect of a Mold Insert

Based on the 3D scanning results, it can be seen that the deposition process of the two core inserts, FDAC and SKD61, was different. Contrary to the initial predictions, the SKD61 core insert tended to bulge in the center after 300 shots, as shown in Figure 10. In contrast, the FDAC core insert had the exact displacement that was initially predicted; the insert was concave in the center, as shown in Figure 9.

Furthermore, because the displacement tended to be concave, the product during the casting process of the FDAC mold cavity appeared burred in the middle of the product, as shown in Figure 15.

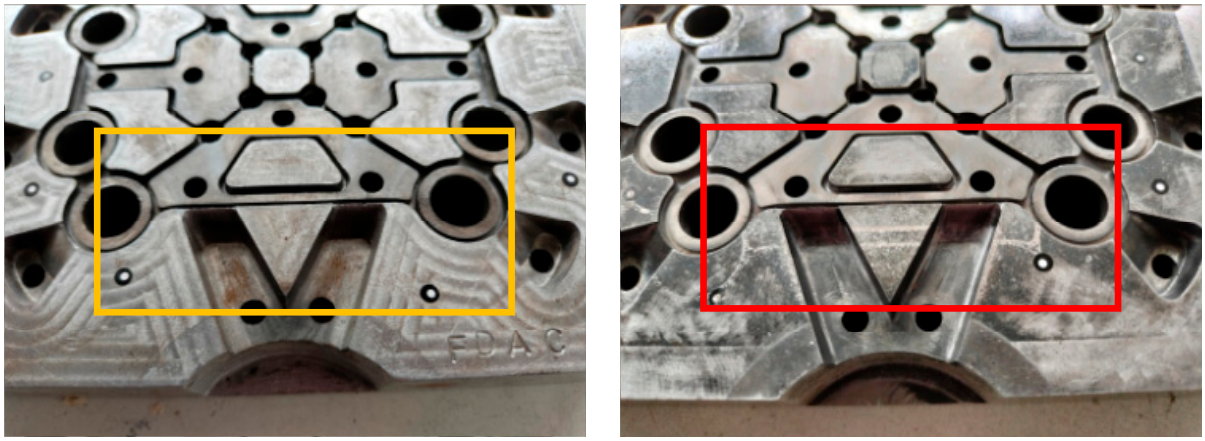


Figure 15. Actual image of corrosion of two core inserts after 300 shots.

There was erosion in the SKD61 cavity, as shown in Figure 16, but it was insignificant. However, the FDAC cavity showed quite a large level of corrosion, especially where the die material flow passed through it, causing noticeable dents to appear on the surface of the plate. The locations of the eight positioning pins on the cavity insert were deformed; the pin's tip was worn but not critically.

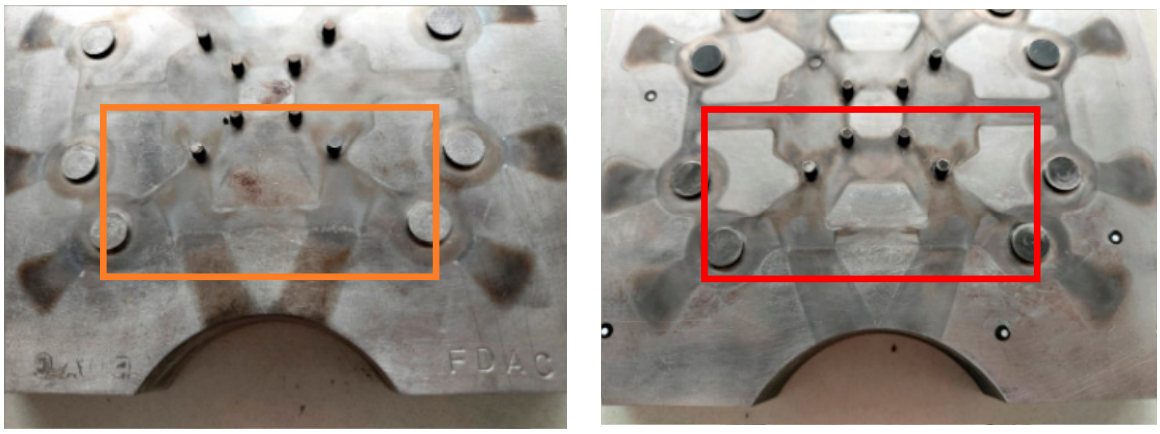


Figure 16. Actual image of abrasion of two cavity inserts. Color frame in Figures 15 and 16 show the area of interest.

During the solidification process of the die material, the molded part demonstrated shrinkage, which was predicted during the simulation process. This resulted in the squeezing and pulling of the eight shaping pins toward the center of the cavity insert. This condition caused the product to be pulled along the movable part of the mold when opening the mold, causing the surface of the molded product to curve, as shown in Figure 16. In addition, because the above situation occurred many times, a shaping pin broke and got stuck in the part while opening the mold. This phenomenon appeared on the SKD61 cavity insert, as shown in Figure 16, contrary to previous predictions that the FDAC cavity insert would be the one that was damaged.

The actual height of the gate was also expanded under the influence of the hot die material flow moving in the mold. According to the 3D scanning data, for the SKD61 core insert, after 300 shots, the gate height expanded by 0.039 mm. Similarly, with the FDAC core insert, the gate height also expanded by 0.062 mm. This difference may have been because the hardness of FDAC steel is lower than that of SDK61 steel. The change data are shown in Figure 17.

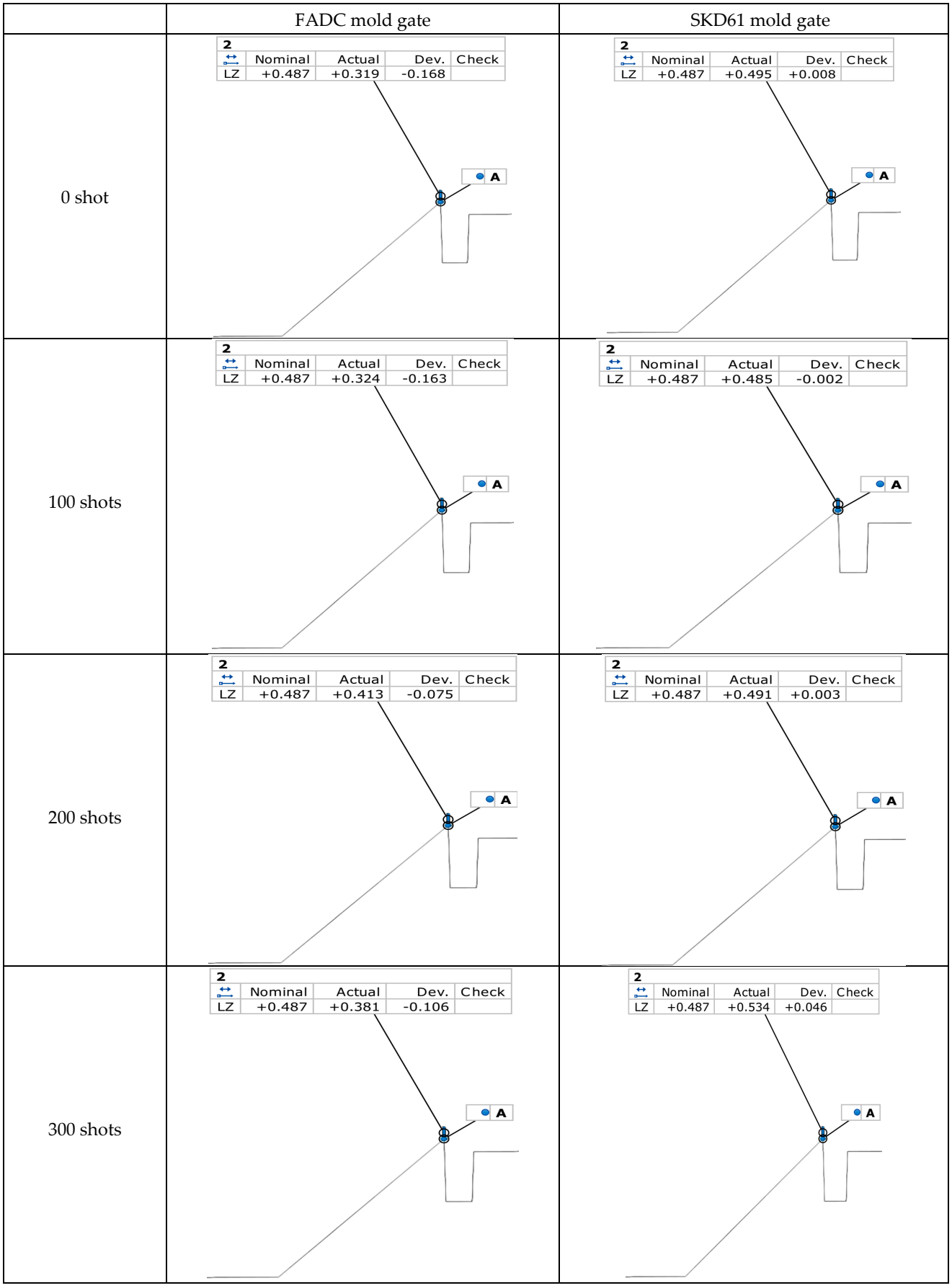


Figure 17. The change in the gate height of FADC and SKD61 core inserts at A as checkpoint, used as reference during 3D-scanning process.

ANOVA is used to evaluate the hypothesis that the means of two or more factors are equivalent. ANOVA is used to determine the significance of one or more factors by comparing the means of the response variable at different factor levels. To determine the statistical significance of any difference between the means, it is necessary to compare the *p*-value with a predetermined significance level α. A significance level of 0.05 represents a 5% probability of incorrectly concluding that there is a difference when, in fact, there is no difference. The F-value is a test statistic used to determine whether a term is related to the response. A high F-value indicates that the term or model is significant [18]. This study used the one-way ANOVA (analysis of variance) method to examine the differences in the deformation of the core inserts with the two types of steel, FDAC and SKD61, after 300 shots. The results indicate that the FDAC steel core inserts had a greater variable value than the SKD61 ones, as shown in Table 3.

Table 3. Variable value between two types of steel.

Materials	**FADC**	**SKD61**
Mean	0.5013	0.3593
Standard Deviation	0.0222	0.0456
Variance	0.000494	0.002075

The formula for the mean is as follows:

$$Mean = \left(\sum x_i\right) / \mathrm{n} \tag{2}$$

where

X_i: value;

n: number of values.

The formula for the standard deviation is as follows:

$$Standard\ Deviation = \frac{\sqrt{\sum (x_i - mean)^2}}{n-1} \tag{3}$$

The formula for the variance is as follows:

$$Variance = \frac{\sum (X_i - Mean)^2}{n-1} \tag{4}$$

However, according to the results from the analysis using the ANOVA method, this difference was not significant enough to conclude that the wear of the two mold cavities, FDAC and SKD61, was different, as shown in Table 3.

A similar analysis was conducted with two cavity inserts composed of FDAC and SKD61 steels. The results were the same as the analysis of the core inserts, indicating that the FDAC steel cavity inserts had a greater variable value than the SKD61 ones.

4. Conclusions

This study assessed the performance of FDAC and SKD61 steel inserts in the high-pressure die-casting (HPDC) process over 300 shots. While both insert types showed some changes, the limited number of casting cycles makes it difficult to draw firm conclusions about their wear differences. Instead, this research emphasizes the variations in the mold cavity's behavior during the casting process. The findings indicate that SKD61 steel was a more durable material, providing better wear resistance and performance in high-stress areas of the mold. On the other hand, FDAC steel, despite experiencing more wear and

deformation, remains a cost-effective choice for less-demanding applications due to its lower cost and ease of machining. Compared to the FDAC mold, the SKD61 mold had a far stronger wear resistance, with maximum deposition values of only 0.009 mm, or 25%.

By combining computational simulations, experiments, and 3D scanning, this study offers valuable insights into wear patterns, dimensional stability, and thermal fatigue behavior. SKD61′s enhanced durability and resistance position it as the preferred option for improving product quality and extending tool life in HPDC molds. The results highlight the importance of material selection and surface treatments in enhancing the lifespan and performance of mold inserts under high-pressure conditions. Future research should aim to increase the number of casting cycles to understand the long-term wear and fatigue effects better.

Author Contributions: Conceptualization, H.N.L.D. and X.T.V.; formal analysis, H.N.L.D., V.H.H. and X.T.V.; funding acquisition, H.N.L.D. and X.T.V.; investigation, H.N.L.D., V.-T.N., X.T.V. and V.T.T.N.; project administration, H.N.L.D. and X.T.V.; visualization, H.N.L.D., V.H.H. and X.T.V.; writing—original draft, H.N.L.D., V.-T.N. and X.T.V.; writing—review and editing, H.N.L.D., V.-T.N. and V.T.T.N. All authors have read and agreed to the published version of the manuscript.

Funding: The authors thank the support of the HCMC University of Technology and Education (HCMUTE) via grant no. T2024-09 for this study.

Data Availability Statement: The data used to support the findings of this study are available from the corresponding author upon request.

Acknowledgments: We would like to thank Ho Chi Minh City University of Technology and Education for supporting this research.

Conflicts of Interest: The authors declare no conflicts of interest.

References

1. Bonollo, F.; Gramegna, N.; Timelli, G. High-Pressure Die-Casting: Contradictions and Challenges. *JOM* **2015**, *67*, 901–908. [CrossRef]
2. Guo, Z.-P.; Xiong, S.-M.; Liu, B.-C.; Li, M.; Allison, J. Effect of Process Parameters, Casting Thickness, and Alloys on the Interfacial Heat-Transfer Coefficient in the High-Pressure Die-Casting Process. *Met. Mater. Trans. A* **2008**, *39*, 2896–2905. [CrossRef]
3. Domkin, K.; Hattel, J.; Thorborg, J. Modeling of high temperature- and diffusion-controlled die soldering in aluminum high pressure die casting. *J. Mech. Work. Technol.* **2009**, *209*, 4051–4061. [CrossRef]
4. Queudeville, Y.; Ivanov, T.; Nußbaum, C.; Vroomen, U.; Bührig-Polaczek, A. Decision and Design Methodologies for the Lay-Out of Modular Dies for High-Pressure-Die-Cast-Processes. *Mater. Sci. Forum* **2009**, *618–619*, 345–348. [CrossRef]
5. Piekło, J.; Garbacz-Klempka, A.; Burbelko, A. The Numerical Fatigue Life Analysis of a Conformal HPDC Mould Core Additively Manufactured from Maraging Steel. *Materials* **2022**, *16*, 365. [CrossRef] [PubMed]
6. Patria, H.; Susanto, I.; Belyamin, B.; Kamal, D.M. Enhancing side die resistance to thermal shock in automotive casting: A comparative study of FCD550 and SKD6 materials. *East.-Eur. J. Enterp. Technol.* **2024**, *3*, 46–55. [CrossRef]
7. Mayer, A.R.; de Oliveira, W.R.; Fals, H.D.C.; Lima, M.J.; Gonçalves, C.S.; Munoz, N.; Corso, J.L.; Pukasiewicz, A.G.M. Die soldering and corrosion failure of high temperature tool steel for high-pressure die casting Al alloy. *Eng. Fail. Anal.* **2024**, *161*, 108314. [CrossRef]
8. Nunes, V.; Silva, F.; Andrade, M.; Alexandre, R.; Baptista, A. Increasing the lifespan of high-pressure die cast molds subjected to severe wear. *Surf. Coat. Technol.* **2017**, *332*, 319–331. [CrossRef]
9. Oudin, A.; Penazzi, L.; Rézaï-Aria, F. Life prediction of hot work tool steels subjected to thermomechanical fatigue. *Mater. Tech.* **2000**, *88*, 67–72. [CrossRef]
10. Tsai, F.; Yan, B.; Kuan, C.; Huang, F. A Taguchi and experimental investigation into the optimal processing conditions for the abrasive jet polishing of SKD61 mold steel. *Int. J. Mach. Tools Manuf.* **2008**, *48*, 932–945. [CrossRef]
11. Chen, S.-H.; Gao, M.-S. The study of chip characteristics and tool wear in milling of SKD61 mold steel. *J. Mech. Sci. Technol.* **2022**, *36*, 2817–2824. [CrossRef]
12. Majerník, J.; Podařil, M.; Gojdan, D. Influence of Overflow Connecting Channel Cross-Section Design on Selected Parameters of High Pressure Die Casting. *Arch. Foundry Eng.* **2020**, *21*, 75–80. [CrossRef]

13. Yeh, S.-H.; Chiu, L.-H.; Chuang, T.-L.; Wu, C.-Y. Thermal Fatigue Behavior Evaluation of Shot-Peened JIS SKD61 Hot-Work Mold Steel. *Mater. Trans.* **2013**, *54*, 1053–1056. [CrossRef]
14. Evaluation of an Arterial Calcification Score as a Predictive Factor of Anastomotic Leakage in Right Colectomy. Case Medical Research. July 2019. Available online: https://www.centerwatch.com/clinical-trials/listings/NCT04002921/evaluation-of-an-arterial-calcification-score-as-a-predictive-factor-of-anastomotic-leakage-in-right-colectomy?page=3&country=France&city=Plerin (accessed on 13 April 2025).
15. Sun, Y.-H.; Yan, H.; Xiong, J.-J. Al_3Ti/ADC12 Composite Synthesized by Ultrasonic Chemistry in Situ Reaction. *Sci. Eng. Compos. Mater.* **2020**, *27*, 10–18. [CrossRef]
16. Frings, M.; Berkels, B.; Behr, M.; Elgeti, S. Comparison of optimization algorithms for the slow shot phase in HPDC. In Proceedings of the 21st International ESAFORM Conference on Material Forming: ESAFORM 2018, Pelermo, Italy, 23–25 April 2018; p. 110005.
17. Fajkiel, A.; Dudek, P.; Reguła, T. Mechanical Properties of Magnesium Die Castings Produced Utilizing Process Scrap. *Arch. Foundry Eng.* **2014**, *14*, 31–34. [CrossRef]
18. Yang, W.-C.; Yang, J.-Y.; Kim, R.-C.; Jon, G.-H.; Chadha, U. Approximate formulas for quality index Q_0 of cast aluminum alloys according to mechanical tensile properties using multiple linear and quadratic regression models. *Int. J. Interact. Des. Manuf. (IJIDeM)* **2023**, *18*, 7365–7380. [CrossRef]

Disclaimer/Publisher's Note: The statements, opinions and data contained in all publications are solely those of the individual author(s) and contributor(s) and not of MDPI and/or the editor(s). MDPI and/or the editor(s) disclaim responsibility for any injury to people or property resulting from any ideas, methods, instructions or products referred to in the content.